analytical chemistry

Article

pubs.acs.org/ac

Nanoparticle-Enhanced Laser-Induced Breakdown Spectroscopy of Metallic Samples

A. De Giacomo,*[,†,‡] R. Gaudiuso,[†,‡] C. Koral,[†] M. Dell'Aglio,[‡] and O. De Pascale[‡]

[†]Department of Chemistry, University of Bari, Via Orabona 4, 70126 Bari, Italy

[‡]IMIP-CNR, Via Amendola 122/D, 70126 Bari, Italy

ABSTRACT: In this article, an increase of 1−2 orders of magnitude in laser-induced breakdown spectroscopy (LIBS) signals was obtained by depositing silver nanoparticles on metal samples. Nanoparticle-enhanced LIBS (NELIBS) was found to be a robust and flexible tool for the chemical analysis of metals because the sample emission signal did not appear to be affected much by the size and concentration of deposited nanoparticles (NPs) within the ranges of 10 nm for diameter and 1 order of magnitude for concentration. On the other hand, preliminary NELIBS tests on insulators and semiconductors did not show any significant enhancement with respect to conventional LIBS. In this article, we present a detailed investigation of the fundamental features of NELIBS spectra, in addition to some examples of analytical applications to the quantitative analysis of metal alloys.

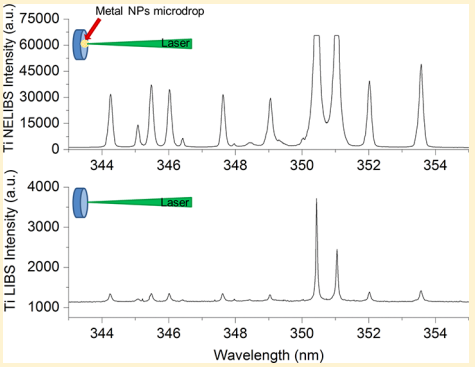

Laser-induced breakdown spectroscopy (LIBS) has been widely used in modern analytical chemistry because it offers a series of advantages such as fast response, no or minimal sample treatment, and easy setup.[1−3] The sensitivity of LIBS depends on the elements, with the limit of detection (LOD) generally varying between a few and 100 ppm for most conventional instruments. Many techniques have been proposed for enhancing the sensitivity of LIBS, most of which involve specific instrumental arrangements, such as double-pulse LIBS[4,5] or resonance LIBS.[6] In this article, we propose a method based on the deposition of silver nanoparticles (Ag NPs) on the sample surface to improve the LOD by 1−2 orders of magnitude.

With respect to the LIBS techniques mentioned above, which require complex experimental setups and expensive equipment, the proposed method has several advantages. Specifically, it requires minimal treatment of the sample; is extremely simple and inexpensive; and does not necessitate any modifications of the experimental setup, so that it can be employed directly with commercial LIBS systems.

Impurities and microflakes on the surface are well-known to decrease the breakdown threshold because of their lower thermal conductivities and small dimensions, which are, in turn, responsible for locally increasing the laser irradiance.[7,8] Moreover, when two different solids are put into contact upon laser irradiation, the solid with the lowest breakdown threshold provides seed electrons that locally increase the temperature in the contact zone.[7,9] These advantages are strongly enhanced if nanoparticles deposited on the target surface are employed to lower the breakdown threshold.[9,10] This is because NPs significantly increase the laser−matter interaction surface and NPs themselves can be considered as extremely efficient thermally insulated defects and excellent electron sources, as the breakdown threshold of metallic NPs is much lower than that of bulk metals. As a consequence, they can provide several points of plasma ignition that, in turn, can cause more efficient ablation. A complete description of NP−laser interactions is still the subject of discussion in the scientific community and beyond the scope of this article, which is instead focused on the application of metal NPs for optical emission enhancement in LIBS and for improving the analytical performance of the technique in terms of sensitivity and LOD in metal target analysis.

In the present work, a drop of colloidal dispersion is deposited on the sample surface, so that, when the solvent evaporates, NPs remain adhered to the surface and change its properties, notably lowering the breakdown threshold as discussed above. Recently, other approaches exploiting the addition of NPs to samples were investigated. In ref 11, a difference in the LIBS signals of bulk and nanostructured ZnO samples was observed and indicated an increase of the signal in the latter case. Another approach was proposed for the LIBS analysis of leaves covered by a thin layer of colloidal solutions,[12] for which an increase of 3−5 times was found for the intensity of the spectral lines. In this work, nanoparticle-enhanced LIBS (NELIBS) has been studied from the fundamental and application points of view to develop an analytical procedure to enhance the emission intensities of elements contained in the metallic matrix without any changes in the experimental configuration.

Received: May 30, 2013
Accepted: October 3, 2013
Published: October 3, 2013

EXPERIMENTAL SETUP

In this work, a typical LIBS apparatus was used, consisting of a laser source for ablation and plasma induction and a spectrograph for optical emission spectroscopy.[1] A Q-switched Nd:YAG laser (Quanta System, model Giant 770-10) with energy up to 1.8 J/pulse and a pulse duration of 8 ns at 1064 nm was used as the laser source. The system for radiation detection comprises a monochromator with a spectral range from 250 to 750 nm and a 1800 groove/mm grating (Jobin Yvon Horiba TRIAX 550) coupled with an intensified charge-coupled device (ICCD) (Jobin Yvon Horiba CCD-3000). A digital delay/pulse generator (Stanford Research Systems, model DG535) was used to synchronize the plasma production and the emission spectra acquisition by setting the gate width, T_g, and delay time, T_d, of the ICCD aperture. The laser pulse was focused on the target by a lens of 100-mm focal length. The emitted light was reflected by an aluminum mirror of 50-mm diameter, and the reflected beam was collected through a 75-mm-focal-length biconvex UV fused-silica lens directly on the monochromator entrance slit. The position of the collecting mirror was changed according to the experiment that was being performed. To maximize the signal for performing chemical analysis, the mirror was placed with a collection angle of about 82° with respect to the incident laser direction. On the other hand, to determine the species spatial distribution with spectral resolved image acquisition, the mirror was placed at a 45° angle with respect to the incident laser.

Each emission spectrum was acquired in single-shot mode. Before each LIBS measurement, a set of cleaning laser shots (three to five) was focused on the sample to keep the surface conditions similar among different experiments. In the case of NELIBS, a drop of Ag colloidal solution was deposited on the sample surface after the preparation laser shots had been applied. A standardized adjustable-volume micropipette was used to place 0.5-μL drops of 20-nm certified spherical Ag NP dispersions (0.02 mg/mL in aqueous buffer, Sigma-Aldrich) on the target surface. The solution was then evaporated to form a homogeneous coating layer of NPs on a circular area of 2-mm radius. To investigate the effect of particle size on NELIBS enhancement, different sets of experiments were performed using certified spherical Ag NP dispersions (0.02 mg/mL in aqueous buffer, NanoComposix, Inc.) of both 20- and 10-nm particle sizes, as well as Ag NPs of different sizes produced by laser ablation in liquid, as described in ref 13. The calculated surface concentration on the sample was 32 ng cm^{-2}. The employed substrates were metals and alloys (Ti and Cu, Goodfellow; Pb, Advent), certified copper-based alloys (L3 and B21 from TechLab; SN1, SN2, SN3, TB2, and TB3 from MBH Analytical LTE), certified steel (C8 from BAM), commercial galvanized steel, a fragment of the Sikhote Alin iron meteorite, Teflon, and silicon wafer.

RESULTS AND DISCUSSION

Basic Aspects of NELIBS. A representative example of the differences occurring between conventional LIBS and NELIBS is presented in Figure 1, where it is shown that, for a titanium target, most lines in the NELIBS spectrum are increased by more than 2 orders of magnitude.

To understand the main causes of this phenomenon, the laser-induced breakdown threshold was measured for pure samples and Ag-NP-covered samples. To estimate systematically the breakdown event, the onset of light emission was monitored both by a photodiode and by naked eye. The threshold fluence was considered as the lowest laser pulse energy producing a statistically reproducible plasma emission event. Results for a set of samples are reported in Table 1 and show that, for metals, a decrease of the breakdown threshold occurs, ranging from 19% to 35%, whereas no difference occurs for silicon and Teflon.

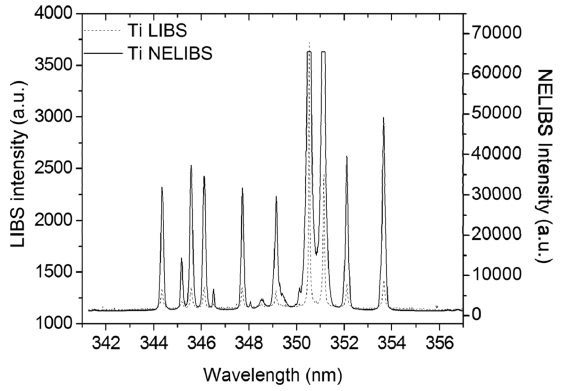

Figure 1. Comparison between LIBS and NELIBS spectra of pure Ti, displaying enhancement factors of 1−2 orders of magnitude. The acquisition conditions were as follows: T_d = 800 ns, T_g = 200 ns, laser fluence = 10 J/cm^2.

Table 1. Comparison between Breakdown Thresholds of Solid Targets with and without Ag NPs

sample	LIBS (J/cm^2)	NELIBS (J/cm^2)	threshold difference (%)
copper	1.42	0.96	33
titanium	1.02	0.66	35
iron	1.17	0.87	26
silicon (amorphous)	3.11	3.11	–
Teflon	3.74	3.74	–
C8 (steel)	1.20	0.89	27
B21 (bronze)	1.31	1.06	19
L3 (brass)	1.46	1.14	22

To understand the effect of the threshold decrease on the plasma emission at laser pulse energies typically used in LIBS chemical analysis, we acquired temporally and spectrally resolved images with the experimental configuration described in detail in refs 5 and 14. As an example, a frame of a spectrally resolved image is reported in Figure 2. It is worth noting that this image should not be considered for measuring the enhancement because it is not spatially integrated and has very high temporal resolution, but on the contrary, it really show the spatial distribution of the emitting species along the propagation axis. Figure 2 compares a set of spectrally resolved images at a 1.4-μs delay time as obtained by LIBS and NELIBS of a copper target, with a 100-ns gate width. Figure 2 shows that the plasma dynamics changes in the NELIBS case. The latter question appears interesting, as it suggests that a higher amount of material is ejected in NELIBS than in conventional LIBS. It is also noteworthy that, in the case of NELIBS, the emission signal at 328.07 nm of Ag I, coming from NPs, has a spatial distribution similar to those of the elements from the bulk target. Figure 3 displays the position along the plasma propagation axis of the maximum of the spatial distribution of the Cu I line at 334.93 nm, as determined by spectrally resolved

dx.doi.org/10.1021/ac4016165 | Anal. Chem. 2013, 85, 10180−10187

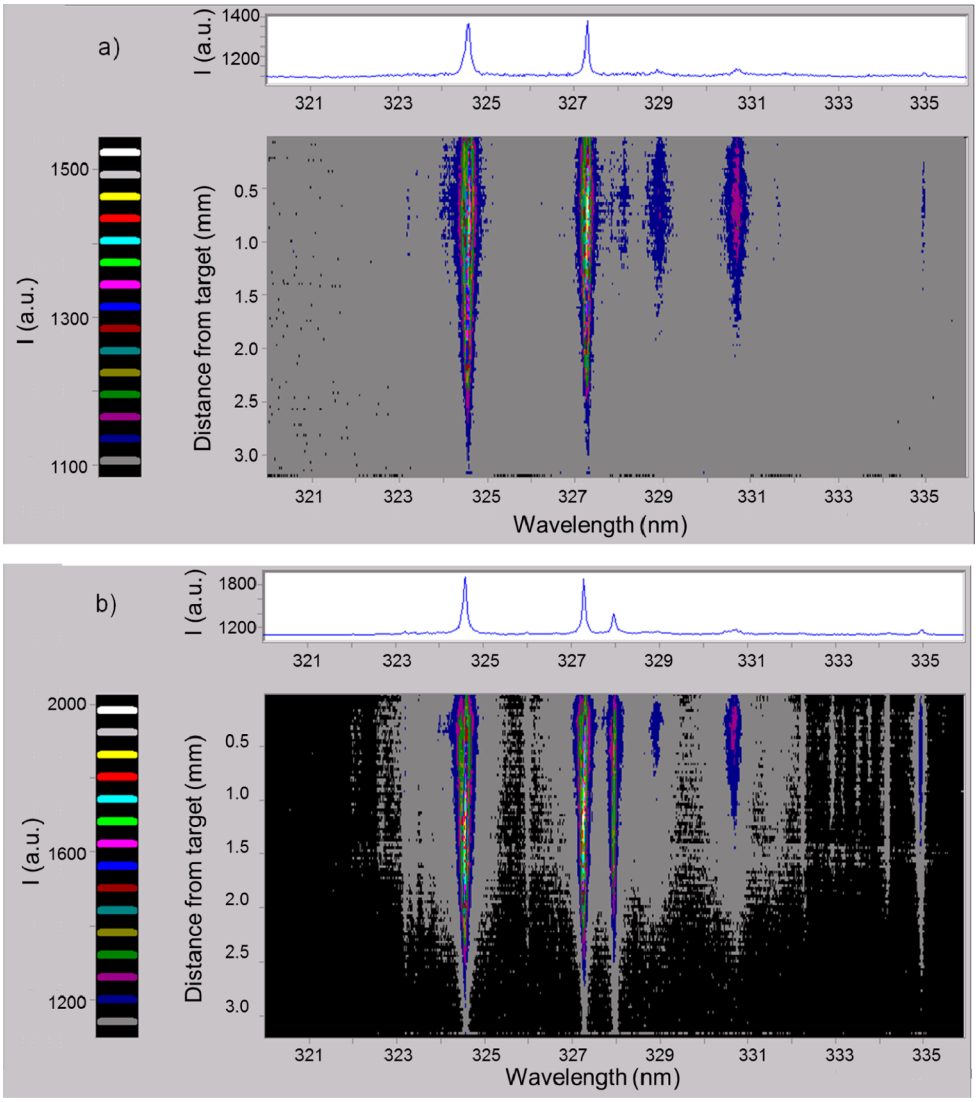

Figure 2. Spectrally resolved images of (a) Cu LIBS and (b) Cu NELIBS plasma. The acquisition conditions were as follows: T_d = 1.4 μs, T_g = 100 ns, laser fluence = 47 J/cm^2.

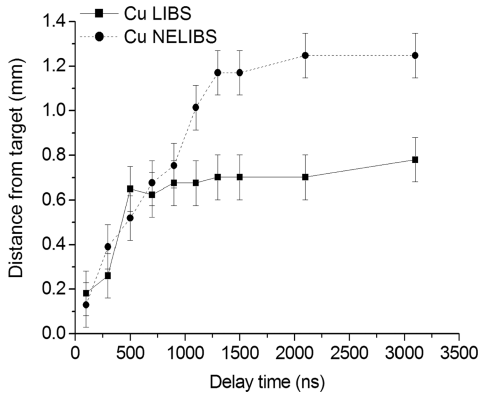

Figure 3. Spatiotemporal distribution of the Cu I line at 334.93 nm in time-resolved LIBS and NELIBS experiments. The acquisition conditions were as follows: T_d = 0−3000 ns, T_g = 100 ns, laser fluence = 47 J/cm^2.

images and plotted as a function of the delay time after the laser pulse, during the ablation of a pure copper target for both LIBS and NELIBS. The graph shows the typical laser-induced plasma dynamics, where the plasma is initially characterized by high number density and high temperature and experiences free expansion, compressing the surrounding air. As a consequence of the plasma expansion and the induction of a shockwave that is driven in the surrounding air, the plasma remains confined within a characteristic distance from the irradiated sample portion.[15] This distance depends on the background conditions and the amount of ablated material.[16] In this case, the background conditions are the same (i.e., air at normal conditions), so the longer persistence and larger emitting volume of the plasma produced by NELIBS with respect to normal LIBS is mainly due to the more efficient ablation, in agreement with the decrease of the ablation threshold observed for metals.

As an example, the temperature and electron number density of the plasma, determined with a Boltzmann plot[17,18] and Stark broadening,[17,19] respectively, are reported in Figure 4 for the NELIBS and LIBS of pure titanium. Figure 4 shows that the plasma parameters exhibit virtually the same trend in both cases and throughout most of the expansion, in agreement with ref 11. The decreasing trend of electron number density, in both cases, is consistent with the well-known recombination

dx.doi.org/10.1021/ac4016165 | Anal. Chem. 2013, 85, 10180−10187

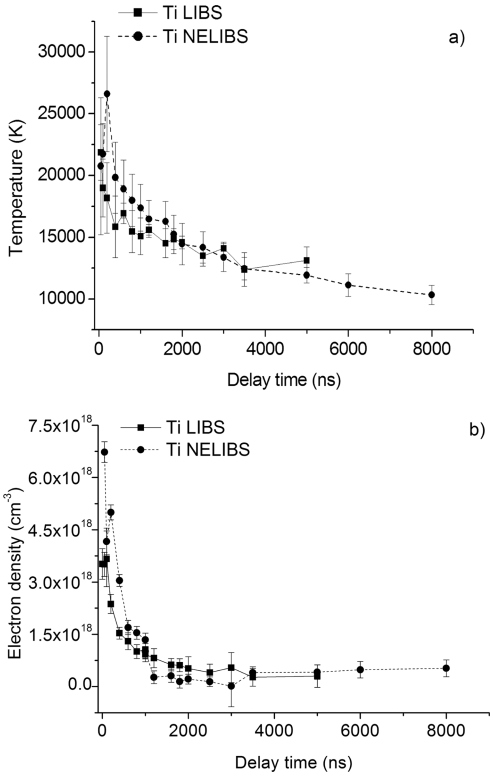

Figure 4. Temporal evolution of plasma parameters in LIBS and NELIBS of pure Ti. The acquisition conditions were as follows: T_d = 0−8000 ns, T_g = 200 ns, laser fluence = 4 J/cm^2.

character of laser-induced plasmas.[20] The only significant difference is correlated with the longer duration of the plasma observed in all NELIBS experiments. It is nevertheless beneficial to stress that, as usual in LIBS studies, data at short delay should be considered with caution as a consequence of self-absorption.[21,22]

Because we established that the NELIBS enhancement can be mainly ascribed to a decrease in the ablation threshold and because it is well-known that the breakdown thresholds of micro- and nanoparticles depend on their size, we studied the effect of the Ag NP size on the NELIBS spectra. This effect was investigated in a restricted size range using colloidal dispersions of NPs with diameters in the range of 10−20 nm, and the results are reported in Figure 5. This figure shows that the emission intensity of the elements of the target is almost unaffected by the dimensions of the Ag NPs, which suggests that a strictly monodisperse solution is not necessary for the analytical application of NELIBS. In Figure 6, the intensities of the four Fe I lines shown in the spectra of Figure 5 are reported as a function of the concentration of the colloidal solution. Figure 6 shows clearly that the emission intensity of elements in the target is virtually unaffected by the Ag NP concentration and that it is randomly distributed around the average value, at least in the considered concentration range. This implies that the analysis can be performed with a rather straightforward sample preparation, without the necessity of controlling the exact concentration of the solution or the volume of the drop to be deposited on the sample surface, and this represents an important practical advantage of the NELIBS technique. It is interesting, however, to emphasize that, whereas the concentration and size of the Ag NPs do not appear to be crucial for the analysis of the bulk sample elements by NELIBS, the LIBS

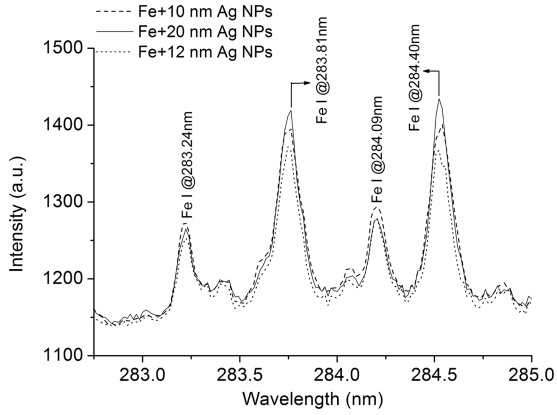

Figure 5. Comparison between NELIBS spectra of steel with Ag NP dispersions of 10-, 12-, and 20-nm diameter. The acquisition conditions were as follows: T_d = 800 ns, T_g = 4 μs, laser fluence = 4 J/cm^2.

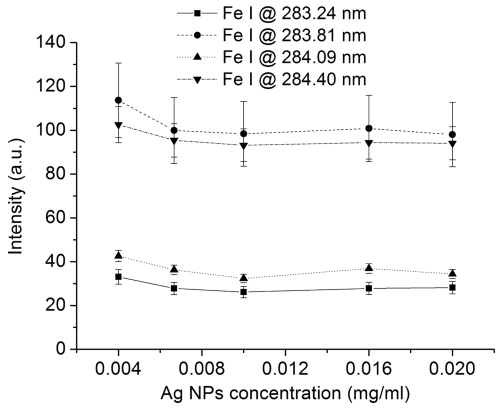

Figure 6. Dependence of the emission intensities of four Fe I transitions during NELIBS of steel with Ag NP dispersions of different concentration and 20 nm of diameter. The acquisition conditions were as follows: T_d = 800 ns, T_g = 4 μs, laser fluence = 4 J/cm^2. The error bars are due to the fitting procedure of the peaks shown in Figure 5.

signal of Ag NPs themselves is extremely sensitive to these two factors.[23,24] As an example, Figure 7 presents the Ag I LIBS

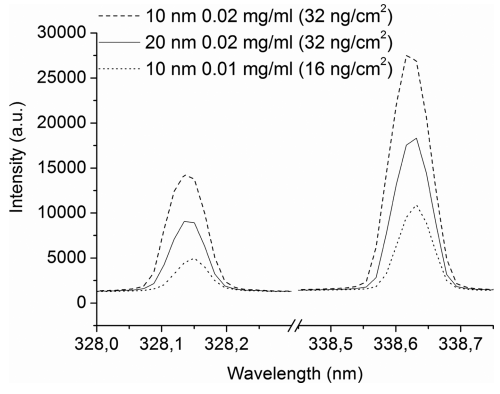

Figure 7. Dependence of the Ag I emission intensity during LIBS of Ag NPs deposited on Si from dispersions of different dimensions and concentrations. (The concentrations of NPs in solution are expressed in mg/mL, and the surface concentrations after deposition on the solid substrates, reported in parentheses, are expressed in ng/cm^2.) The acquisition conditions were as follows: T_d = 800 ns, T_g = 10 μs, laser fluence = 5 J/cm^2.

dx.doi.org/10.1021/ac4016165 | Anal. Chem. 2013, 85, 10180−10187

spectra of Ag NPs with different diameters and concentrations, deposited on a silicon wafer have instead rather different intensities. In Figure 7, the LIBS signal of the NPs appears to vary consistently with the change in concentration of 10-nm NPs and to be affected as well by the particle size when the concentration of Ag atoms is kept constant. These results suggest that the interaction of the NPs with these kinds of substrates is negligible and that low-threshold NPs are preferentially ablated.

NELIBS was also tested with a set of high-threshold samples such as insulators (including a basalt mineral, a soil sample, and a Teflon pellet) and a semiconductor (i.e., silicon). The results reported in Table 1 show negligible difference in the ablation threshold with and without Ag NPs, and conversely, no significant enhancement is observed for the LIBS signal. It is interesting to note that, when the enhancement of lines from elements of the sample is high, the signal of silver coming from the NPs is low, whereas the opposite occurs when the sample signal is not enhanced, as in the case of the insulator and semiconductor. For the latter samples, the signal of atomic silver coming from the NPs is extremely high, which suggests that, if quantitative analysis of NP solutions is pursued, the use of this type of substrate is strongly recommended. Figure 8 exemplifies this phenomenon, showing the Ag I spectral line at 328.07 nm for the NELIBS of Teflon, where no emission enhancement was detected for the elements of the sample, and of copper, where an enhancement of about 50 times the conventional LIBS signal was observed. The two spectra reported in Figure 8 confirm that an inverse proportionality exists between the emission enhancement of elements from the target and the intensity of the Ag I signal from the NPs.

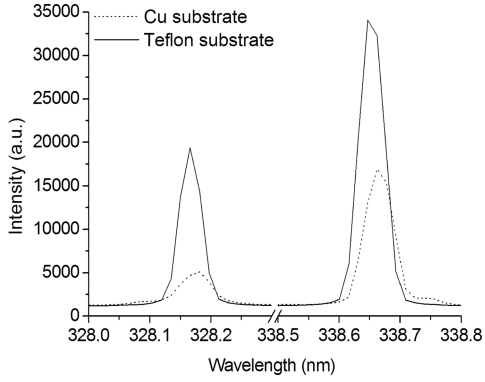

Figure 8. Dependence on the kind of substrate of the emission intensity of Ag atoms coming from deposited NPs. The acquisition conditions were as follows: laser fluence = 46 J/cm^2, time-integrated measurement.

Analytical Approach. NELIBS with Ag NPs was tested on different metallic alloys, namely, steel, bronze, and brass, whose enhanced and conventional spectra are shown in Figure 9. On a more quantitative basis, Figure 10 presents a comparison between the calibration lines obtained by LIBS and NELIBS for Mn and Pb in copper-based alloys. The advantages of applying NELIBS are evident in terms of signal enhancement and sensitivity improvement, as shown by the 55 and 33 times increases achieved for the slopes of the Mn and Pb calibration lines, respectively. These results imply an LOD decrease of more than 1 order of magnitude for these elements under the employed experimental conditions.

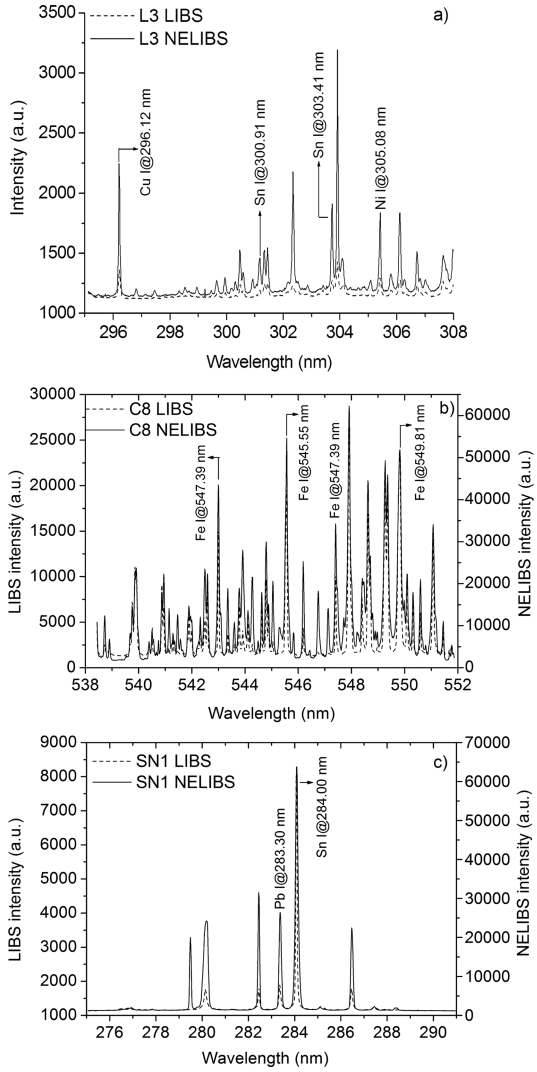

Figure 9. Comparison between LIBS and NELIBS spectra of three certified metal alloys: (a) brass L3, (b) steel C8, and (c) bronze SN1. The acquisition conditions were as follows: T_d = 1 μs, T_g = 5 μs, laser fluence = 13 J/cm^2 for L3; T_d = 1.5 μs, T_g = 10 μs, laser fluence = 23 J/cm^2 for C8; T_d = 1 μs, T_g = 4 μs, laser fluence = 9 J/cm^2 for SN1.

Figure 11 shows three noteworthy cases in which the use of NELIBS enabled the detection of emission lines of low-concentration elements that, under the employed experimental conditions, were not visible in the conventional LIBS spectra. A particularly interesting result is the one obtained for the detection of iridium in iron meteorites[25] and reported in Figure 11c for the Sikhote Alin meteorite, which contains 0.024 ppm of Ir.[26] The figure shows that the Ir I line at 266.48 nm in the LIBS spectrum is below the LOD and that it becomes clearly visible in the NELIBS spectrum. Despite these important advantages connected to the improvement of element detection in analytical applications, NELIBS can introduce two drawbacks that should be mentioned here. The first is related to sample contamination by the metallic NPs. The importance of this question was estimated for different metallic targets by focusing a set of pulses on the sample surface, after the single-shot NELIBS measurement, to measure how many shots were necessary to completely remove the Ag NPs from the sample itself. This investigation was carried out by monitoring the intensity decrease of the Ag I signal at 328.07 nm as a function

dx.doi.org/10.1021/ac4016165 | Anal. Chem. 2013, 85, 10180−10187

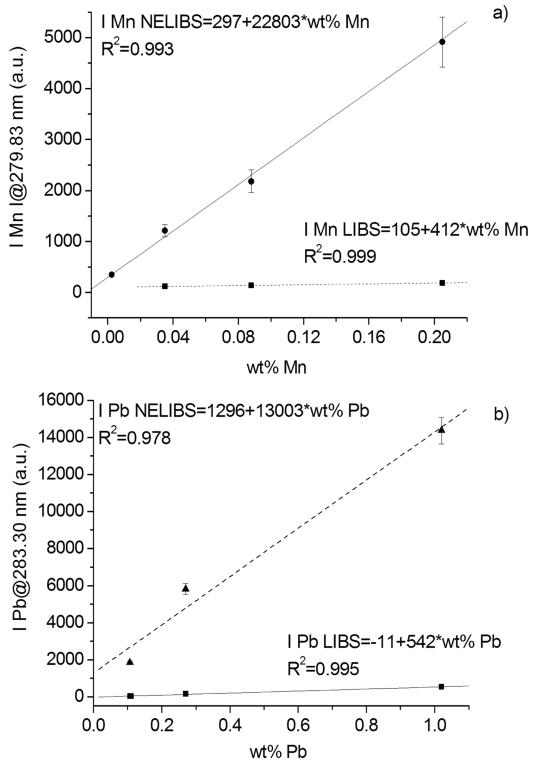

Figure 10. Comparison between the LIBS and NELIBS calibration lines of (a) Mn and (b) Pb contained in copper-based alloys. The acquisition conditions were as follows: T_d = 1 μs, T_g = 1.5 μs, laser fluence = 7 J/cm^2. The samples employed for the Mn line and for the Pb line were L3, TB2, TB3, and SN3.

of the number of laser shots. The results are shown in Figure 12 for various targets and indicate that, with the exception of the lead target, Ag NPs are removed after a few shots. In the case of lead, the complete removal of Ag NPs occurs after more than 100 shots as a consequence of the low melting point of this metal and of the embedding of NPs during the resolidification phase after the laser shot. The second disadvantage is due to the possible spectral interference of the emission lines of the NP element with the transitions of the elements of the target. This effect can be avoided by selecting suitable lines of the sample and taking into account the transitions of the NP metal, for example, by acquiring a spectrum of the pure metal or of the NPs themselves deposited on a noninteracting substrate. Moreover, by changing the type of NP, this drawback can be completely eliminated. As an example, we present in Figure 13 the LIBS and NELIBS spectra of an Al-based alloy with NPs of different metals. In this case, Ag NPs could not be used, because of the spectral interference between the Al I and Ag I transitions, so Au and Cu NPs that we produced by liquid-phase laser ablation[13] were used instead. Our laboratory-produced NPs were characterized by surface-plasmon resonance (SPR) absorption, which, for the Au NPs, indicated an average size in the range of 5−10 nm.[27] The Cu NPs, on the other hand, could not be precisely characterized because they undergo immediate oxidization in water.[27] Nonetheless, Figure 13 clearly shows that a significant intensity enhancement of the Al I emission lines is provided by both types of NPs. Based on these results, it appears that, for metals, the phenomenon of LIBS emission enhancement with NPs of different types is general, although a dependence of its extent on the type of NP can be expected.

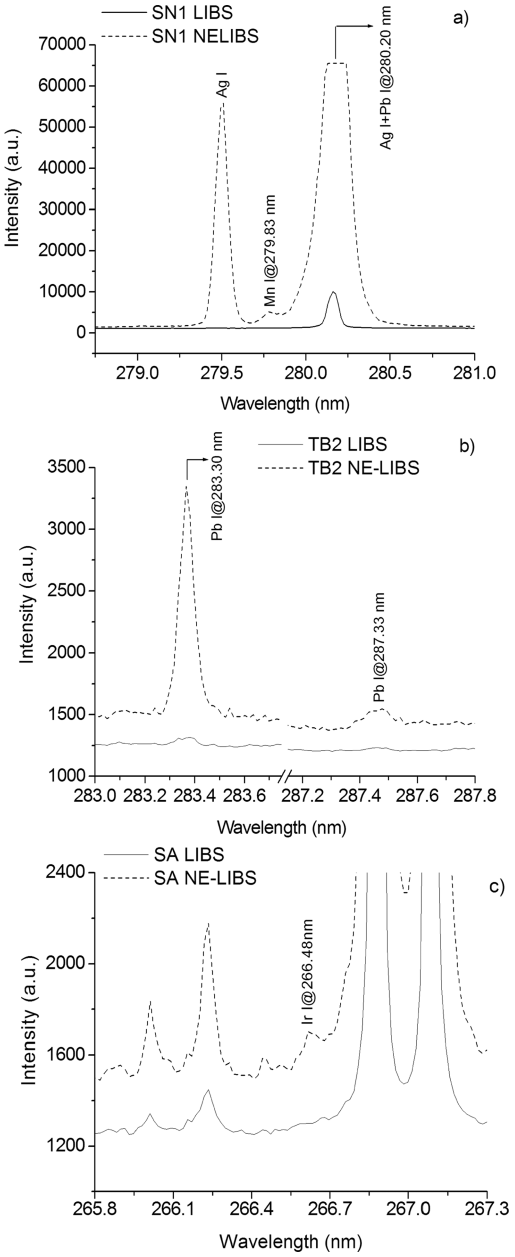

Figure 11. Details of LIBS and NELIBS spectra of (a) a tin bronze (SN1), (b) a brass (TB2), and (c) an iron meteorite (Sikhote Alin, SA). The acquisition conditions for the spectra of the copper-based alloys were as follows: T_d = 1 μs, T_g = 4 μs, laser fluence = 9 J/cm^2. The acquisition conditions for the spectra of the iron meteorite were as follows: T_d = 1 μs, T_g = 10 μs, laser fluence = 46 J/cm^2.

CONCLUSIONS

In this article, we have proposed a variant of conventional LIBS based on the use of metallic NPs to enhance the emission intensity of solid targets (nanoparticle-enhanced LIBS, NELIBS). NELIBS appears to be able to provide a very straightforward method to improve LIBS sensitivity, as it requires only trivial sample treatment and no change in the instrumental setup. Indeed, this technique is merely based on the deposition of a drop of noble-metal colloidal solution on the surface of the sample to be analyzed, and the induced contamination can be completely removed after a few laser shots. We showed that the main causes of the NELIBS enhancement are related to changes in the ablation process,

dx.doi.org/10.1021/ac4016165 | Anal. Chem. 2013, 85, 10180−10187

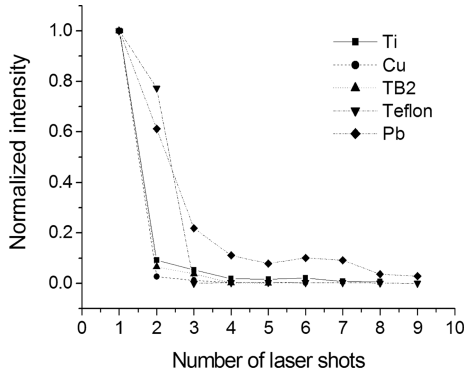

Figure 12. Decrease of Ag emission intensity as a function of the number of laser shots focused on different targets to remove deposited NPs. The acquisition conditions were as follows: laser fluence = 46 J/cm^2, time-integrated measurement.

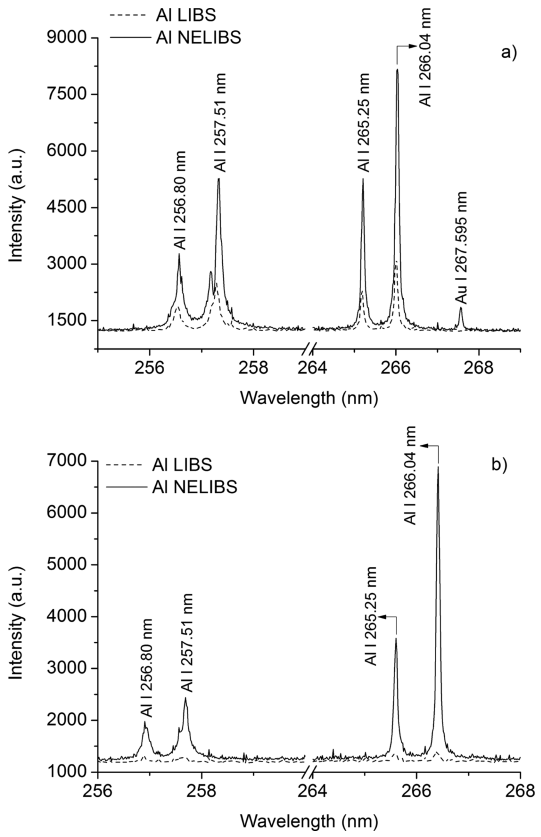

Figure 13. LIBS and NELIBS spectra of an Al-based alloy with (a) AuNPs and (b) CuNPs. The acquisition conditions were as follows: T_d = 1 μs, T_g = 1.5 μs, laser fluence = 22 J/cm^2.

because a significant decrease in the ablation threshold was detected for all of the investigated metal samples. Moreover, an increase in the amount of material ejected during NELIBS was observed by acquiring spectrally resolved images to investigate the dynamics of the plasma induced during LIBS and NELIBS. On the other hand, virtually no difference was observed in the LIBS and NELIBS plasma parameters (i.e., temperature and electron number density). The obtained enhancement appeared to be dependent on the kind of ablated sample, reaching up to 1−2 orders of magnitude in the case of metallic targets and remaining essentially negligible in the case of high-threshold samples such as insulators and semiconductors. It is worth emphasizing that laser ablation can inherently suffer from matrix effects and differential vaporization of some elements. It is not straightforward whether these phenomena can be avoided by the deposition of NPs on the target surface, so the cautions normally used for laser ablation-based techniques should also be taken into account for NELIBS.

AUTHOR INFORMATION

Corresponding Author

*E-mail: alessandro.degiacomo@ba.imip.cnr.it.

Notes

The authors declare no competing financial interest.

ACKNOWLEDGMENTS

This research was partially supported by MIUR (PRIN Project 2010ERFKXL_007). The authors acknowledge Remah ElRashedy for taking part in the experiments and scientific discussion.

REFERENCES

(1) Miziolek, A. W., Palleschi, V., Schechter, I., Eds. *Laser Induced Breakdown Spectroscopy*; Cambridge University Press: New York, 2006.
(2) Hahn, D. W.; Omenetto, N. *Appl. Spectrosc.* **2010**, *64/12*, 335A−366A.
(3) Omenetto, N. *J. Anal. Atom. Spectrom.* **1998**, *13*, 385−399.
(4) Babushok, V. I.; De Lucia, F. C., Jr.; Gottfried, J. L.; Munson, C. A.; Miziolek, A. W. *Spectrochim. Acta B* **2006**, *61*, 999−1014.
(5) De Giacomo, A.; Dell'Aglio, M.; Bruno, D.; Gaudiuso, R.; De Pascale, O. *Spectrochim. Acta B* **2008**, *63/7*, 805−816.
(6) Goueguel, C.; Laville, S.; Vidal, F.; Sabsabi, M.; Chaker, M. *J. Anal. Atom. Spectrom.* **2010**, *25*, 635−644.
(7) Radziemski, L. J., Cremers, D. A., Eds. *Laser-Induced Plasmas and Applications*; Marcel Dekker: New York, 1989, and references therein.
(8) Walters, C. T.; Barnes, R. H.; Beverly, R. E., III. *J. Appl. Phys.* **1978**, *49*, 2937−2949.
(9) Jang, H. W.; Sands, T.; Lee, J. L. *J. Appl. Phys.* **2003**, *94*, 3529−3535.
(10) Ye, J. Y.; Balogh, L.; Norris, T. B. *Appl. Phys. Lett.* **2002**, *80*, 1713−1715.
(11) El Sherbini, A. M.; Aboulfotouh, A. M.; Rashid, F. F.; Allam, S. H.; El Dakrouri, A.; El Sherbini, T. M. *World J. Nano Sci. Eng.* **2012**, *2*, 181−188.
(12) Ohta, T.; Ito, M.; Kotani, T.; Hattori, T. *Appl. Spectrosc.* **2009**, *63/5*, 555−558.
(13) De Giacomo, A.; Dell'Aglio, M.; Santagata, A.; Gaudiuso, R.; De Pascale, O.; Wagener, P.; Messina, G. C.; Compagnini, G.; Barcikowski, S. *Phys. Chem. Chem. Phys.* **2013**, *15*, 3083−3092.
(14) De Giacomo, A.; Dell'Aglio, M.; Gaudiuso, R.; Cristoforetti, G.; Legnaioli, S.; Palleschi, V.; Tognoni, E. *Spectrochim. Acta B* **2008**, *63/9*, 980−987.
(15) De Giacomo, A.; Dell'Aglio, M.; Gaudiuso, R.; Amoruso, S.; De Pascale, O. *Spectrochim. Acta B* **2012**, *78*, 1−19.
(16) Bogaerts, A.; Chen, Z. *Spectrochim. Acta B* **2005**, *60*, 1280−1307.
(17) Griem, H. R. *Principles of Plasma Spectroscopy*, Cambridge University Press: New York, 1997.
(18) Fauchais, P.; Coudert, J. F., Sardelle, M. Diagnostics in thermal plasma processing. In *Plasma Diagnostics*; Anciello, O., Flamm, D. L., Eds.; Academic Press: New York, 1989; Vol. *1*, Chapter 7.
(19) Konjevic, N. *Phys. Rep.* **1999**, *316*, 339−401.
(20) De Giacomo, A. *Spectrochim. Acta B* **2011**, *66*, 661−670.
(21) Quintero, M. C.; Rodero, A.; Garcia, M. C.; Sola, A. *Appl. Spectrosc.* **1997**, *51*, 778−784.
(22) Moon, H. Y.; Herrera, K. K.; Omenetto, N.; Smith, B. W.; Winefordner, J. D. *Spectrochim. Acta B* **2009**, *64*, 702−713.
(23) Diwakar, P. K.; Loper, K. H.; Matiaske, A. M.; Hahn, D. W. *J. Anal. Atom. Spectrosc.* **2012**, *27*, 1110−1119.

(24) Dewalle, P.; Sirven, J. B.; Roynette, A.; Gensdarmes, F.; Golanski, L.; Motellier, S. *J. Phys. Conf. Ser.* **2011**, *304*, 012012.
(25) Dell'Aglio, M.; De Giacomo, A.; Gaudiuso, R.; De Pascale, O.; Senesi, G. S.; Longo, S. *Geochim. Cosmochim. Acta* **2010**, *74*, 7329−7339.
(26) Wasson, J. T.; Huber, H.; Malvin, D. J. *Geochim. Cosmochim. Acta* **2007**, *71*, 760−781.
(27) Burakov, V. S.; Butsen, A. V.; Tarasenko, N. V. *J. Appl. Spectrosc.* **2010**, *77*, 386−393.